

# Multicriteria Optimization of the Trajectory Tracking Filtering Procedure by Genetic Algorithm

Dmitrii A. Bedin

N.N. Krasovskii Institute of Mathematics and Mechanics  
of the Ural Branch of the Russian Academy of Sciences  
(IMM UB RAS)  
Ekaterinburg, Russia  
bedin@imm.uran.ru  
ORCID: 0000-0002-3790-2943

Alexey G. Ivanov

N.N. Krasovskii Institute of Mathematics and Mechanics  
of the Ural Branch of the Russian Academy of Sciences  
(IMM UB RAS)  
Ekaterinburg, Russia  
iagsoft@imm.uran.ru  
ORCID: 0000-0002-5852-7273

**Abstract**—For the Interacting Multiple Model (IMM) method of trajectory tracking, a genetic optimization procedure is proposed that optimizes its internal parameters. For trajectory filtering, the quality of the algorithm is determined by not one but multiple criteria. The proposed optimization algorithm makes it possible to improve and identify Pareto-optimal solutions.

**Keywords**—trajectory tracking, filtering problem, Interacting Multiple Model method, multi-objective optimization genetic algorithms, Pareto optimality

## I. TRAJECTORY TRACKING PROBLEM

An observed object (an aircraft) moves according to the dynamics:

$$\dot{x} = f(t, x) \quad (1)$$

where  $x$  is the state vector. For the needs of navigation in air traffic control (ATC), the following simple version of aircraft dynamics is often used [1]:

$$\begin{cases} \dot{x}_N(t_i) = V(t_i) \cos \varphi(t_i), \\ \dot{x}_E(t_i) = V(t_i) \sin \varphi(t_i), \\ \dot{V}(t_i) = w(t_i), \\ \dot{\varphi}(t_i) = u(t_i)/V(t_i). \end{cases} \quad (2)$$

Here,  $x_N$  and  $x_E$  are the north and east aircraft coordinates,  $V$  is the velocity magnitude,  $\varphi$  is the course angle; the controls  $w$  and  $u$  are the longitudinal and lateral accelerations;  $t_i$  is the current time instant. The motion system (2) with  $u(t) = w(t) = 0$  is called the constant velocity (CV) model [1], [2]. The section where  $u(t) = \text{const}$  and  $w(t) = 0$  corresponds to the coordinated turn (CT) model, the section where  $u(t) = 0$  and  $w(t) = \text{const}$  is the constant acceleration (CA) section.

Surveillance devices such as radars, GNSS, bearing- and distance-measurement systems make measurements at discrete instants  $t_i$ :

$$y_i = h(t_i, x(t_i)) + \omega_i. \quad (3)$$

Here,  $\omega_i$  is the random measurement error. For many measuring systems (radars, GNSS), the function  $h$  simply selects the “geometric” part of the coordinates ( $x_N$ ,  $x_E$ ) of the state vector  $x$ .

The trajectory tracking filtering problem is the problem of making an estimate  $\hat{x}_i$  of the state vector  $x(t_i)$  at  $t_i$  as the function (or algorithm) of the measurement history up to the time instant  $t_i$ :  $\hat{x}_i = \hat{x}(\{y_j : j \leq i\})$ .

In the case where dynamics (1) and observation equation (3) are linear and the measurement errors  $\omega_i$  are Gaussian, the Kalman filter [3] is the best estimator of the state vector that minimizes the mean squared error

$$J(t_i) = E\{(\hat{x}_i - x(t_i))^2\} \quad (4)$$

If dynamics (1) has “switches” in time (for example, in dynamics (2), the controls  $u(t)$  and  $w(t)$  have the piecewise-constant structure), the Kalman filter is not optimal.

For the motion with the switching dynamics (2), the behavior of criterion (4) as a function of time  $t$  along the trajectory can vary greatly depending on the filtering algorithm [2]. For example, as a rule, algorithms that provide a small value of  $J$  in time segments of long-term constancy of the controls  $u(\cdot)$  and  $w(\cdot)$  have a large peak of  $J$  values at the instant of switching the controls  $u(\cdot)$ ,  $w(\cdot)$ . The opposite is also observed: algorithms that have a small peak at the time of changing the controls have the worst  $J$  in the segments of constancy.

Algorithms based on the hidden Markov models (HMM) show quite balanced behavior (the relative smallness of the criterion  $J(t_i)$  in all sections of the aircraft motion) [4]. The Interacting Multiple Model (IMM) method [2], [4], which is based on HMM and includes several Kalman filters with different motion models, is the mostly implemented in ATC systems algorithm.

The IMM method has a large number of parameters that affect the quality of its work [2], [4]. The most important thing is which and how many dynamics models are included in its structure. With a fixed set of dynamics models, the process of switching between them is very important. The switching is governed by the transition probability matrix. Its elements (or the constants on which they depend) are the second important tuning set of parameters. Also, the parameters are important that define the behavior of each model, including the noise level of the dynamics.

The authors set the problem of adjusting the parameters of the IMM algorithm in order to improve the quality of its work [6]–[8]. It is important to note that the influence of

parameters on the work of the IMM method is complex. In addition, the authors think of changing the number of models in the future. Hence, both real-valued and integer parameters will appear in the problem. Therefore, the authors decided to use direct search methods for optimization. The genetic approach, which is a direct search with heuristics [5] (each individual in the population of the genetic algorithm corresponds to a fixed set of the IMM parameters), seemed to be the most convenient option and was implemented by the authors [6]–[8].

## II. TRAJECTORY TRACKING QUALITY CRITERIA

An important feature of the problem under consideration is that, in practical trajectory tracking, it is usual to use other criteria rather than the criterion  $J$  to assess the quality of the trajectory tracking work. These criteria describe the proximity between the true state  $x(t_i)$  and its estimate  $\hat{x}_i$  in different senses. In air traffic control, the quality of trajectory approximation is evaluated in “channels” and motion sections. The quality requirements are summarized in standards [9], [10].

The trajectory of the aircraft is divided into sections, i.e., the intervals of constancy (CV, CT, CA) of the controls  $u(\cdot)$  and  $w(\cdot)$  in system (2), as well as the sections of stabilization after the change of controls [9].

Channels are scalar indicators [9] that characterize the deviation vector  $x(t) - \hat{x}$ : the longitudinal  $\delta_{lon}$  and lateral  $\delta_{lat}$  deviations and the deviations in the velocity magnitude  $\delta_V = V(t) - \hat{V}$  and the course angle  $\delta_\varphi = \varphi - \hat{\varphi}$ . The longitudinal and lateral deviations are expressed by the formulas:

$$\begin{aligned}\delta_{lon} &= \cos\varphi(t)(x_N(t) - \hat{x}_N(t)) + \sin\varphi(t)(x_E(t) - \hat{x}_E(t)), \\ \delta_{lat} &= -\sin\varphi(t)(x_N(t) - \hat{x}_N(t)) + \cos\varphi(t)(x_E(t) - \hat{x}_E(t)).\end{aligned}$$

Standards [10] set the upper limits of the root-mean-square (RMS) deviations in the channels separately for the sections of constant controls and for the maximum deviations during the control switching sections. These values depend on the “observation scheme”: the number of radars, the time step of measurement income, and the level of the error  $\omega$ . The observation scheme is strictly prescribed in standards [10].

In order to make the criteria suitable for different observation schemes and different maneuvering capabilities of the aircraft, it was decided to compare the deviations  $\delta$  not with the standard, but with the Cramér-Rao lower bound (CRLB) [11, 12]. The Cramér-Rao lower bound sets the lower bound for the mean square of the deviation of the unbiased estimates  $\hat{x}$ . It can be calculated using dynamics (2) and the controls  $u(\cdot)$  and  $w(\cdot)$ . In our case, it is a  $4 \times 4$  matrix with the elements  $R_{NN}$ ,  $R_{NE}$ , .... The computational formulas for  $R(t)$  as a function of time  $t$  are based on the formulas from [12] applied to dynamics (2).

The absolute deviations  $\delta$  are converted into the relative deviations  $\Delta$  by dividing by the corresponding value of the CRLB:

$$\begin{aligned}\Delta_{lon} &= \delta_{lon} / \sqrt{\cos^2\varphi(t)R_{NN} + 2\sin\varphi\cos\varphi R_{NE} + \sin^2\varphi R_{EE}}, \\ \Delta_{lat} &= \delta_{lat} / \sqrt{\sin^2\varphi(t)R_{NN} + 2\sin\varphi\cos\varphi R_{NE} + \cos^2\varphi R_{EE}}, \\ \Delta_V &= \delta_V / \sqrt{R_{VV}}, \quad \Delta_\varphi = \delta_\varphi / \sqrt{R_{\varphi\varphi}}.\end{aligned}$$

After this transformation, the deviations  $\Delta$  become not only universal relative to different observation schemes, but also surely applicable to different motion sections: at the switches of the controls  $u$  and  $w$ , the CRLB  $R(t)$ , as well as an estimate  $\hat{x}(t)$ , has a peak and, after the switch, it has a stabilization section [8]. Due to this property, in our algorithm, instead of the criteria from standards [10], we apply other criteria based on the relative deviations  $\Delta$ .

In our optimization program, the deviations  $\delta$  and  $\Delta$  are calculated along each trajectory from the training set. Then we calculate the criteria: the RMS deviations in the channels  $c_{lon}$ ,  $c_{lat}$ ,  $c_V$ , and  $c_\varphi$ , as well as the combined RMS deviations  $c_{2d}$  in the plane  $(x_N, x_E)$  and  $c_{4d}$  over the entire state vector. The calculation for the one-dimensional channel criterion is performed according to the following formula (the example is for  $c_{lon}$ ):

$$c_{lon} = \sqrt{\frac{1}{n} \sum_{k=1}^N \sum_{i=1}^{n_k} \Delta_{lon}^2(t_i^k)},$$

where  $N$  is the number of trajectories in the training set,  $n_k$  is the number of measurements in the  $k$ th trajectory,  $n = \sum_{k=1}^N n_k$ , and  $t_i^k$  is the instant of the  $i$ th measurement in the  $k$ th trajectory. The multidimensional criteria  $c_{2d}$  and  $c_{4d}$  are calculated by to the following formulas:

$$\begin{aligned}c_{2d} &= \sqrt{\frac{1}{n} \sum_{k=1}^N \sum_{i=1}^{n_k} \delta_{2d}^T(t_i^k) R_{2d}^{-1}(t_i^k) \delta_{2d}(t_i^k)}, \\ c_{4d} &= \sqrt{\frac{1}{n} \sum_{k=1}^N \sum_{i=1}^{n_k} \delta_{4d}^T(t_i^k) R^{-1}(t_i^k) \delta_{4d}(t_i^k)},\end{aligned}$$

where  $\delta_{2d} = [\delta_{lon} \delta_{lat}]^T$ ,  $\delta_{4d} = [\delta_{lon} \delta_{lat} \delta_V \delta_\varphi]^T$ , and  $R_{2d}$  is the left upper  $2 \times 2$  block of the matrix  $R$ .

Since the estimates  $\hat{x}$  are affected by random measurement errors  $\omega$ , the values of the criteria  $c_{lon}$ ,  $c_{lat}$ , ..., calculated using the set of trajectories are random numbers themselves. To correctly handle them, the genetic program calculates the confidence intervals for  $c_{lon}$ ,  $c_{lat}$ , .... The calculation procedure is presented in [8].

## III. THE PARETO FRONT CALCULATION

In trajectory tracking, algorithms with sufficiently small values of different quality criteria are needed for practical use. The criteria may be contradictory: for example, an improvement in the criterion  $c_V$  in the velocity channel may lead to a worse estimation of the coordinates on the plane and higher values of the criterion  $c_{2d}$ . Simulations confirm this fact: it was observed that the values of the parameters

optimal for each criterion do not coincide and are often quite far from each other.

The search for parameters that are simultaneously good for different criteria, but not necessarily optimal according to any criterion, closely echoes the search for Pareto-optimal points. Therefore, the authors decided to introduce the determination of a Pareto front into the existing [6]–[8] genetic optimization algorithm. For this purpose, the nondominated sorting algorithm from [13] was used.

It should be noted that there is a range of genetic optimization algorithms (including NSGA-II described in [13]) initially focused on multi-criteria optimization [14] and special processing of the Pareto-optimal individuals in the selection procedures. The authors withheld the transition to such algorithms, since the existing genetic algorithm [6]–[8] seems suitable for finding the Pareto-optimal solutions.

The nondominated sorting algorithm ranks the population by assigning different ranks to the individuals. Rank 1 corresponds to the Pareto-optimal individuals. Rank 2 is for the individuals that become Pareto-optimal after the removal of the individuals of rank 1, etc. The ranks, on the one hand, show the proximity of the solution to Pareto optimality and, on the other hand, allow us to visualize the processes within the genetic optimization. For example, the mutation (non-directed breeding) has the goal of diversifying the population as much as possible, and, during the mutation, we should expect the appearance of individuals with different ranks. The selection procedure should leave the “correct” (from a practical standpoint) individuals in the population, and it is expected that, as a result of its work, individuals with a high rank will be preserved.

Such properties of the genetic procedures were demonstrated in the simulations. During the work, the computations were performed on the Uran supercomputer at the IMM UB RAS. The maximum population size was 4,000 individuals. The training set consisted of 2000 model trajectories with dynamics (2) with different observation schemes and maneuverable capabilities of the aircraft. The modeling technique is described in detail in [7], [8].

Figs. 1–3 show the projections of the population on the plane of the two criteria. Fig. 1 presents two criteria  $c_{lat}$  and  $c_{lon}$ , which reflect the quality of the trajectory filtering in the horizontal plane. There is a weak “correlation” between the values of the criteria within the population. Individuals of rank 1 are placed in the lower left corner as if they are Pareto-optimal only for these two criteria. The color of the remaining individuals gradually changes from green to blue in accordance with the rank in the direction from the lower left corner to the upper right corner. Fig. 2 shows the projection of the population on the plane of the criteria  $c_\phi$  and  $c_V$ . In contrast to Fig. 1, there is no “correlation” between the criteria, while the distribution of ranks is different: Pareto-optimal solutions are located among other solutions in the middle of the figure. This is due to the fact that the figure is a projection of a complex spatial picture, and individuals with “average” quality values of the criteria  $c_\phi$  and  $c_V$  have very good values of the rest.

In all Figs. 1–3, the diversity of the population is noticeable: there are many individuals with different criteria values and different ranks. Fig. 3 presents the same plane of

two criteria  $c_V$  and  $c_\phi$  as in Fig. 2, but shows only those individuals that “survived” after all the generations of the selection process. It can be seen that only individuals of rank 1 and 2 remain; thus, the current selection procedure really selects Pareto-optimal solutions or points close to them.

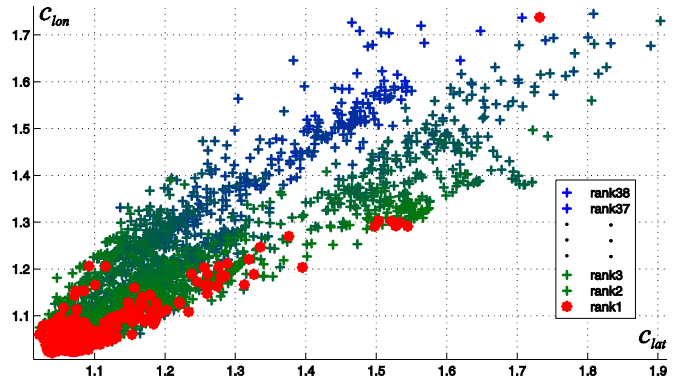


Fig. 1. The projection of the genetic algorithm population onto the plane of the criteria  $c_{lon}$  and  $c_{lat}$

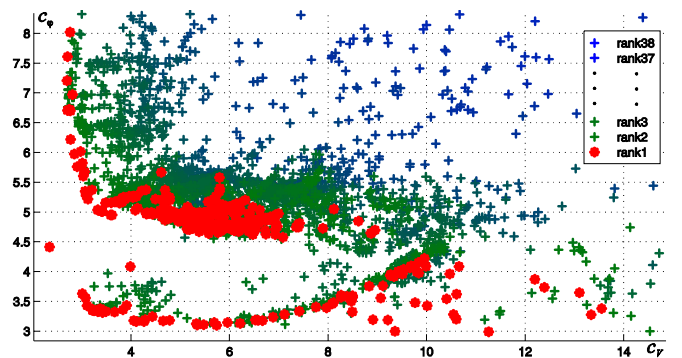


Fig. 2. The projection of the genetic algorithm population onto the plane of the criteria  $c_\phi$  and  $c_V$ .

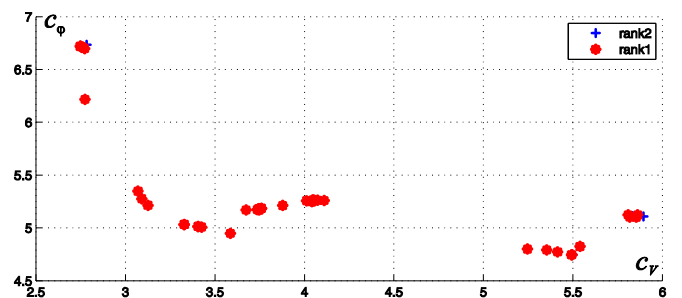


Fig. 3. The projection of the genetic algorithm population onto the plane of the criteria  $c_\phi$  and  $c_V$ . The individuals that “survived” after all the generations of the selection process.

Fig. 4 shows the plane of two genes  $g_{13}$  and  $g_{15}$ , i.e., two different parameters of the IMM method. The individuals are depicted so that the color, as in the figures above, corresponds to their rank. It can be seen that the individuals of different ranks are well “mixed” with each other, including the individuals with rank 1. This means that the Pareto-optimal parameters are very different and there is no concentration of them near some point. The same pattern is seen in Fig. 5 for the other two genes  $g_{11}$  and  $g_{12}$ , but, in contrast to Fig. 4, the entire population as a whole is biased to some more optimal values

## ACKNOWLEDGMENT

The authors thank the NITA, Llc. for the submitted data and discussion of the problem statement.

## REFERENCES

- [1] X. R. Li and V. P. Jilkov, "Survey of maneuvering target tracking. Part I. Dynamic models," *IEEE Trans. Aerosp. Electron. Syst.*, 2003, vol. 39, no. 4, pp. 1333–1364.
- [2] Y. Bar-Shalom and W. D. Blair, Eds., *Multitarget-Multisensor Tracking: Applications and Advances*, vol. III. Norwood, MA: Artech House, 2000.
- [3] A. V. Balakrishnan, *Kalman Filtering Theory*. New York: Springer, 1984; Moscow: Mir, 1988 [in Russian].
- [4] X. R. Li and V. P. Jilkov, "Survey of maneuvering target tracking. Part V. Multiple-model methods," *IEEE Trans. Aerosp. Electron. Syst.*, 2005, vol. 41, no. 4, pp. 1255–1321.
- [5] Z. Michalewicz, *Genetic Algorithms + Data Structures = Evolution Programs*. Berlin: Springer, 1996.
- [6] D. A. Bedin and A. G. Ivanov, "The use of a genetic algorithm for parameter adjustment of the multi-hypothesis aircraft tracking algorithm," in *26th Saint Petersburg International Conference on Integrated Navigation Systems*, St. Petersburg, CSRI Elektropribor, 2019, pp. 144–147.
- [7] D. A. Bedin and A. G. Ivanov, "Trajectory tracking by the interacting multiple model algorithm: Genetic approach to improve the performance," in *2020 IEEE National Radar Conference (RadarConf20)*, Florence, Italy, 2020, pp. 1–6.
- [8] D. A. Bedin and A. G. Ivanov, "Multicriteria genetic optimization procedure for trajectory tracking by the interacting multiple model algorithm," in *Workshop on Mathematical Modeling and Scientific Computing: Focus on Complex Processes and Systems (dedicated to the memory of Nikolai Botkin)*, Munich, Germany, *CEUR Workshop Proceedings*, 2020, vol. 2783, pp. 17–28.
- [9] EUROCONTROL Standard for Radar Surveillance in En-Route Airspace and Major Terminal Areas, Std. [Online]. Available: <https://www.eurocontrol.int/publication/eurocontrol-standard-radar-surveillance-en-route-airspace-and-major-terminal-areas>.
- [10] EUROCONTROL Specification for ATM Surveillance System Performance, Std. [Online]. Available: <https://www.eurocontrol.int/publication/eurocontrol-specification-atm-surveillance-system-performance-esassp>.
- [11] A. A. Borovkov, *Mathematical Statistics*. Moscow: Nauka, 1984 [in Russian]; Amsterdam: Gordon and Breach, 1998.
- [12] M. Šimandl, J. Královec, and P. Tichavský, "Filtering, predictive, and smoothing Cramér–Rao bounds for discrete-time nonlinear dynamic systems," *Automatica*, 2001, vol. 37, no. 11, pp. 1703–1716.
- [13] K. Deb, A. Pratap, S. Agarwal, and T. Meyarivan, "A fast and elitist multiobjective genetic algorithm: NSGA-II," *IEEE Trans. Evol. Comput.*, 2002, vol. 6, no. 2, pp. 182–197.
- [14] E. Zitzler and L. Thiele, "Multiobjective evolutionary algorithms: A comparative case study and the strength Pareto approach," *IEEE Trans. Evol. Comput.*, 1999, vol. 3, no. 4, pp. 257–271.

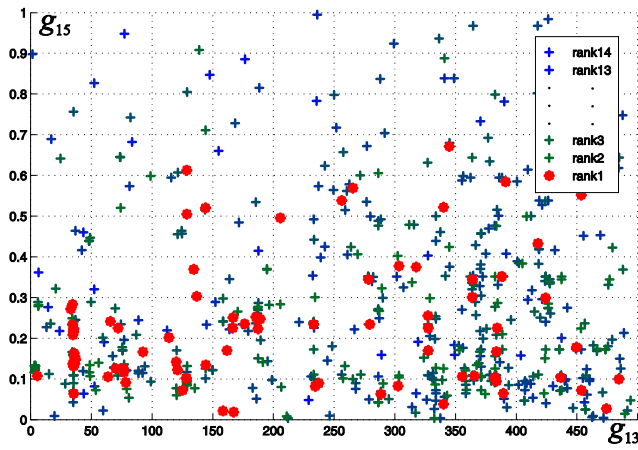


Fig. 4. The projection of the population onto the plane of genes  $g_{13}$  and  $g_{15}$

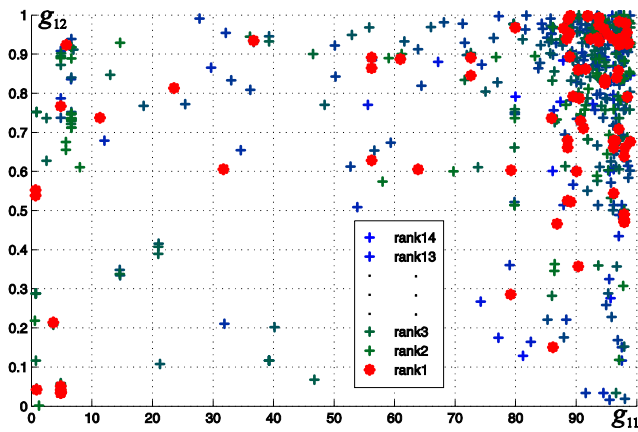


Fig. 5. The projection of the population onto the plane of genes  $g_{11}$  and  $g_{12}$

## IV. CONCLUSION

Using the genetic algorithm in simulations, the authors obtained the parameters of the IMM method that have sufficiently small values of multiple criteria reflecting the requirements of the real trajectory tracking algorithms. Using the nondominated sorting, the Pareto-optimal solutions were identified. In the future, the algorithm can be improved by introducing the priority of individuals with a high rank into the selection procedure.